Mapping Neurotransmitter Networks with PET: An Example on Serotonin and Opioid Systems

Lauri Tuominen,[1,2] Lauri Nummenmaa,[1,3,4] Liisa Keltikangas-Järvinen,[5] Olli Raitakari,[6] and Jarmo Hietala[1,2]*

[1]*Turku PET Centre, University of Turku and Turku University Hospital, Turku, Finland*
[2]*Department of Psychiatry, University of Turku, Turku, Finland*
[3]*Brain Research Unit, O.V. Lounasmaa Laboratory, School of Science, Aalto University, AALTO, Espoo, Finland*
[4]*Department of Biomedical Engineering and Computational Science, School of Science, Aalto University, TKK, Espoo, Finland*
[5]*Department of Behavioral Sciences, University of Helsinki, Helsinki, Finland*
[6]*Research Centre of Applied and Preventive Cardiovascular Medicine, University of Turku and Turku University Hospital, Turku, Finland*

Abstract: All functions of the human brain are consequences of altered activity of specific neural pathways and neurotransmitter systems. Although the knowledge of "system level" connectivity in the brain is increasing rapidly, we lack "molecular level" information on brain networks and connectivity patterns. We introduce novel voxel-based positron emission tomography (PET) methods for studying internal neurotransmitter network structure and intercorrelations of different neurotransmitter systems in the human brain. We chose serotonin transporter and μ-opioid receptor for this analysis because of their functional interaction at the cellular level and similar regional distribution in the brain. Twenty-one healthy subjects underwent two consecutive PET scans using [^{11}C]MADAM, a serotonin transporter tracer, and [^{11}C]carfentanil, a μ-opioid receptor tracer. First, voxel-by-voxel "intracorrelations" (hub and seed analyses) were used to study the internal structure of opioid and serotonin systems. Second, voxel-level opioid–serotonin intercorrelations (between neurotransmitters) were computed. Regional μ-opioid receptor binding potentials were uniformly correlated throughout the brain. However, our analyses revealed nonuniformity in the serotonin transporter intracorrelations and identified a highly connected local network (midbrain–striatum–thalamus–amygdala). Regionally specific intercorrelations between the opioid and serotonin tracers were found in anteromedial thalamus, amygdala, anterior cingulate cortex, dorsolateral prefrontal cortex, and left parietal cortex, i.e., in areas relevant for several neuropsychiatric disorders, especially affective disorders. This methodology enables in vivo mapping of connectivity patterns within and between neurotransmitter systems. Quantification of functional neurotransmitter balances may be a useful approach in etiological studies of neuropsychiatric disorders and also in drug development as a biomarker-based rationale for targeted modulation of neurotransmitter networks. *Hum Brain Mapp 00:000–000, 2013.*

Additional Supporting Information may be found in the online version of this article.

Contract grant sponsors: Academy of Finland; EVO-Funding (Hospital District of Southwest Finland and Turku City); The National Graduate School of Clinical Investigation.

*Correspondence to: Jarmo Hietala, Department of Psychiatry, University of Turku, Kunnallissairaalantie 20, Building 9, 20700-Turku, Finland. E-mail: jahi@utu.fi

Received for publication 19 February 2012; Revised 16 January 2013; Accepted 28 February 2013

DOI: 10.1002/hbm.22298

Published online in Wiley Online Library (wileyonlinelibrary.com).

Key words: serotonin transporter; μ-opioid receptor; positron emission tomography; connectivity; correlation

INTRODUCTION

Positron emission tomography (PET) can be used to quantitatively measure receptor and transporter binding characteristics in various neurotransmitter systems in living human brain. Clinical PET studies typically investigate just one neurotransmitter system at a time. However, dysregulation of several different neurotransmitter systems is practically always implicated in the etiology of neurological and psychiatric disorders. A good example on this is the dopamine and glutamate imbalance theory in schizophrenia [Hirvonen and Hietala, 2011; Marsman et al., 2011]. So far, only a limited number of studies have used PET to directly measure more than one neurotransmitter system at a time and explore correlations of these systems in neuropsychiatric disorders [Bailer et al., 2012; Nakamura et al., 2010]. Moreover, it is evident that dysfunctions of large-scale brain networks rather than differences in single regions underlie psychiatric disorders [Liberzon et al., 2002; Mayberg, 1997; Price and Drevets, 2010]. The term "connectome" coined by Sporns et al. [2005] reflects the importance of appreciating network-level connectivity in order to understand brain function and dysfunction. The "connectome" has been studied from many different perspectives. In vivo anatomical and functional connectivity can be studied with diffusion tensor imaging [Conturo et al., 1999], functional magnetic resonance imaging, and PET [Raichle et al., 2001]. Connectivity patterns in regional neurotransmitter binding have been investigated in the serotonergic system [Erritzoe et al., 2010], and regional networks (striatal and extrastriatal) have been suggested in the dopaminergic system [Cervenka et al., 2010]. Dopaminergic networks were speculated to result from region-specific differences in D2 receptor gene expression demonstrated by Hirvonen et al. [2004, 2009].

Up to date, four PET studies have attempted to describe the interplay of 5-HT_{1A}-receptor and serotonin transporter and one study has examined the correlation between serotonin transporter and 5-HT_{2A} receptor within the serotonin system [Bose et al., 2011; Erritzoe et al., 2010; Jovanovic et al., 2008; Lundberg et al., 2007; Takano et al., 2011]. As far as we know, no imaging study has investigated the functional connectivity of two different neurotransmitter systems in vivo in man. In this study, we explore regional networks within serotonin and μ-opioid systems and relationship between these two neurotransmitter systems.

The serotoninergic pathways include a classical ascending monoamine neurotransmitter system [Moore et al., 1978], whereas μ-opioids are as a rule modulatory peptides with widespread distribution throughout the brain [Sbrenna et al., 2000; Simmons and Chavkin, 1996]. The rationale to study these particular systems is the fact that μ-opioids modulate serotonergic neurotransmission in animal studies [Lopez-Gimenez et al., 2008; Sbrenna et al., 2000; Tao and Auerbach, 1995] possibly thorough μ-opioid receptors located presynaptically in serotonergic neurons [Berger et al., 2006]. Moreover, serotonin and opioid systems regulate similar brain functions, such as pain [Benchenerif et al., 2002; Martikainen et al., 2007] and affect [Liberzon et al., 2002; Meyer, 2007]. Based on the functional interplay of these systems and the possibility that serotonin transporters and μ-opioid receptors are located in the same axon terminals, we hypothesized that μ-opioid receptor binding potentials (BP_{ND}) correlate with serotonin transporter BP_{ND}s.

Here, we introduce and apply a novel data-driven, voxel-wise analysis approach for mapping of the network structure within one neurotransmitter system as well as correlation between the serotonin and opiate systems. Serotonin transporter and μ-opioid receptor were quantified with 3D HRRT PET and highly specific tracers, i.e., [^{11}C]MADAM and [^{11}C]carfentanil, respectively [Frost et al., 1985; Lundberg et al., 2005].

MATERIALS AND METHODS

Subjects

Twenty-one healthy subjects (10 female, 11 male) aged between 30 and 46 (mean 38) were recruited for the study. Subjects had no history of medical or psychiatric illness as confirmed by medical examination and interview, blood and urine screening, ECG, MRI examination, and SCID-I (Structured Clinical Interview for DSM-IV). All subjects gave written consents and the study protocol was approved by the Joint Ethical Committee of the University of Turku and the Turku University Central Hospital. This study followed the ethical guidelines of the Declaration of Helsinki.

Imaging Procedures

A brain-dedicated high-resolution PET scanner (ECAT HRRT, Siemens Medical Solutions) [Rahmim et al., 2005] was used for PET imaging. Prior to emission scan, Cesium-137 point source transmission was used to obtain tissue attenuation maps by forward projection. These maps were then used for attenuation correction. Data was gathered in list mode and reconstructed into $1.22 \times 1.22 \times 1.22$ mm^3 voxel size images with speed-optimized Ordinary Poisson-OSEM in full 3D reconstruction [Comtat et al., 2004]. During the PET scans, head of the subject was fixed

using an individually molded thermoplastic mask and head movement was measured with Polaris Vicra showing movements within the spatial resolution of the scanner. A T1-weighted MRI scan with $1 \times 1 \times 1$ mm^3 resolution voxel size was obtained from each subject using Philips Gyroscan Intera 1.5 T CV Nova Dual MRI scanner to exclude structural abnormalities and for anatomical reference.

All subjects underwent a PET scan with serotonin transporter tracer [^{11}C]MADAM followed by a PET scan with μ-opioid receptor tracer [^{11}C]carfentanil during the same day using identical head positioning. Both ligands are highly specific for their targets. Affinity of [^{11}C]MADAM for serotonin transporter is 1.65 nM and affinity of [^{11}C]carfentanil for μ-opioid receptor is 0.024 nM. Selectivity of [^{11}C]MADAM for serotonin transporter over norepinephrine transporter is 197 and for serotonin transporter over dopamine transporter is over 606. Selectivity of [^{11}C]carfentanil for μ-opioid receptor over δ-opioid receptor is 138 and for μ-opioid receptor over δ-opioid receptor is 1,792 [Edmond et al., 2002; Maguire et al., 1992]. Preparation of tracers has been described elsewhere [Hirvonen et al., 2009; Tarkiainen et al., 2001]. Tracers were injected as intravenous bolus injections and flushed with saline. The injected dose and mass of [^{11}C]MADAM were 484.5 ± 49.9 MBq and 0.59 ± 0.42 μg and the injected dose and mass of [^{11}C]carfentanil were 423.6 ± 73.9 MBq and 1.08 ± 0.84 μg. Radioactivity of [^{11}C]MADAM was measured for 75 min using 17 frames (3×1 min, 4×3 min, and 10×6 min) and radioactivity of [^{11}C]carfentanil for 69 min using 16 frames (3×1 min, 4×3 min, and 9×6 min).

Image Preprocessing

External motion data monitoring was used to determine the frames with least movement in each scan. At least three consecutive frames were selected for each scan. Frames within this interval were first summed and all the other frames of that scan were then coregistered to the sum of that interval. As any one frame has only limited amount of spatial information and the success of coregistration depends on the spatial information, we used this "source image" approach for "frame-to-frame correction" in order to correct for head motion during the scan. To align the two frame-to-frame corrected dynamic PET images as accurately as possible, following preprocessing steps were done. First, integrated [^{11}C]MADAM image was coregistered to [^{11}C]carfentanil integrated image. An average image of coregistered [^{11}C]MADAM image and original [^{11}C]carfentanil integrated image was then calculated. Resulting average image was then used as a reference image to which both original [^{11}C]MADAM and [^{11}C]carfentanil integrated images were coregistered. The obtained parameters were then used to all the time frames of corresponding frame-to-frame corrected [^{11}C]MADAM and [^{11}C]carfentanil images to create final aligned dynamic PET images. Finally, the MR image was coregistered to the average of the integrated final [^{11}C]MADAM and [^{11}C]carfentanil images. All frame-to-frame corrections and coregistrations were done using linear transformations with SPM2 software (http://www.fil.ion.ucl.ac.uk/spm/). Imadeus software (Version 1.4, Forima Inc., Turku, Finland) was used to manually delineate reference regions on individual T1-weighted transaxial MR images. Cerebellar cortex and occipital cortex were used as reference regions for [^{11}C]MADAM and [^{11}C]carfentanil, respectively.

Parametric BP_{ND} images were calculated using in-house software (http://www.turkupetcentre.net/software/show.php?program=imgbfbp) that applies basis function method to estimate voxel-wise BP_{ND} with simplified reference tissue model (SRTM) [Gunn et al., 1997]. The nonlinear term θ_3 was constrained between 0.06 and 0.6 min^{-1} for both ligands ($\theta_3^{min} \geq \frac{k_2^{min}}{1+BP^{max}} + \lambda_{11-C}$ and $\theta_3^{max} \leq k_2^{max} + \lambda_{11-C}$, where k_2 is the efflux rate constant from the tissue, BP is binding potential, and $\lambda_{11\text{-}C}$ is the decay constant of ^{11}C). These limits were chosen based on real data and Monte-Carlo simulations. SRTM allows estimation of BP_{ND} without arterial input function and also gives robust estimates of the other two rate constants, namely, R1 and k_2 [Lammertsma and Hume, 1996]. SRTM has four assumptions that have to be met. First, there has to be a reference tissue, i.e., an area in the brain virtually devoid of the target molecules that can be used to estimate the nonspecific binding of the ligand. Second, radioactive metabolites do not cross the blood–brain barrier. Third, exchange between free and specifically bound compartments is fast enough so that they can be described as one compartment. Finally, volume of distribution of the free compartment is same for tissue and reference regions. The applicability and validity of SRTM has been shown for both [^{11}C]MADAM [Lundberg et al., 2005] and [^{11}C]carfentanil [Endres et al., 2003].

Parametric images were spatially normalized into MNI-space using linear and nonlinear transformations: Summed PET images were first normalized into an in-house ligand-specific template, and these normalization parameters were subsequently applied to the corresponding parametric images. Normalized parametric images were then resliced into $4 \times 4 \times 4$ mm^3 voxel size. Dimension of these images were $40 \times 48 \times 32$ voxels equaling 61,440 voxels per image. These images were smoothed with 8 mm Gaussian kernel. Finally, the smoothed [^{11}C]MADAM and [^{11}C]carfetanil parametric images were masked with a height threshold >0.2. That is, voxels that had BP_{ND} values below 0.2 were excluded from all statistical analyses. Masking was done in order to remove effects due to nonspecific binding in the correlation analyses described below. Examples of [^{11}C]MADAM and [^{11}C]carfentanil parametric images are shown in Figure 1.

Hub analysis

In order to characterize internal network structure of neurotransmitter systems, correlations from a single voxel

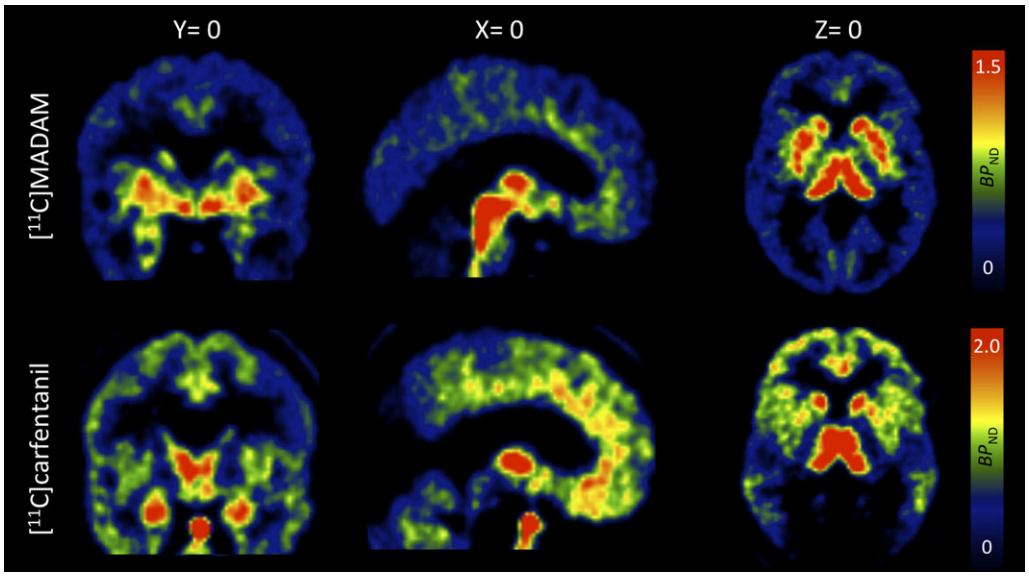

Figure 1.
Examples of [^{11}C]MADAM and [^{11}C]carfentanil parametric BP_{ND} images from the same subject. Images are normalized into MNI space, voxel-size is 2 × 2 × 2 mm^3 and images are smoothed with 2 mm Gaussian kernel. *X*, *Y*, and *Z* denote the MNI-coordinates and color bar indicates voxel-wise BP_{ND}s. [Color figure can be viewed in the online issue, which is available at wileyonlinelibrary.com.]

to all the other voxels within the brain mask were calculated. Then, arithmetic mean of these correlations was computed. This mean correlation coefficient was then written into that voxel to create a new *3D hub image*. This procedure was repeated for all the voxels in the brain. In the resulting *3D hub image*, voxel intensities reflect how strongly the BP_{ND} of each voxel is on average associated with BP_{ND}s elsewhere in the brain. So, for example in the [^{11}C]MADAM hub image, every voxel $X_i = \frac{\sum_{j=1}^{N-1} corr(v_i,v_j)}{N-1}$, where $i = \{1, 2, 3, \ldots, N\}$ is the number of voxels in the image and vectors $v_i = [v_i^1, v_i^2, v_i^3, \ldots, v_i^{21}]$ and v_j $[v_j^1, v_j^2, v_j^3, \ldots, v_j^{21}]$ consist of voxel-wise BP_{ND} values from individual subjects.

This enabled us to localize brain regions that serve as main "hubs" that may determine or control the distribution of the specific neurotransmitter elsewhere in the brain. These analyses were conducted separately for the [^{11}C]MADAM and [^{11}C]carfentanil ligands. Voxel-wise FWE corrected $P < 0.05$ was considered statistically significant.

Seed analysis

Based on the [^{11}C]MADAM hub analysis, we chose five (midbrain, putamen, thalamus, caudate, and amygdala) regions of interest (ROI) and used BP_{ND}s from these regions to predict BP_{ND} elsewhere in the brain using the General Linear Model in SPM2. BP_{ND}s from ROI were extracted using the WFU pickatlas toolbox [Maldjian et al., 2003] and voxels that were not within the hub were excluded from the seed ROIs. Seed analysis was performed in order to further characterize the links from the hub regions to other regions in the brain. Additionally, coefficients of determination for BP_{ND} values between the selected five ROIs were calculated. We did not detect any specific "hubs" in [^{11}C]carfentanil distribution (see below) and therefore no seed analysis was performed for these images. In the seed analysis, voxel-wise FWE corrected $P < 0.05$ was considered statistically significant.

Intercorrelation of [^{11}C]MADAM and [^{11}C]carfentanil

Correlation between [^{11}C]carfentanil and [^{11}C]MADAM ligands was assessed by computing correlations between the BP_{ND}s of [^{11}C]carfentanil and [^{11}C]MADAM in every voxel. Resulting correlation coefficients were written into a new *3D intercorrelation image*, where voxel intensities reflect the voxel-wise correlation between the BP_{ND}s of the two ligands.

RESULTS

Hub Analysis

Hub analysis of [^{11}C]MADAM images revealed a statistically significant cluster (voxel-wise FWE corrected $P < 0.05$, $r > 0.44$) comprising midbrain, thalamus, caudatus, putamen, and amygdala. Hub analysis of [^{11}C]carfentanil images was unable to differentiate any particular region

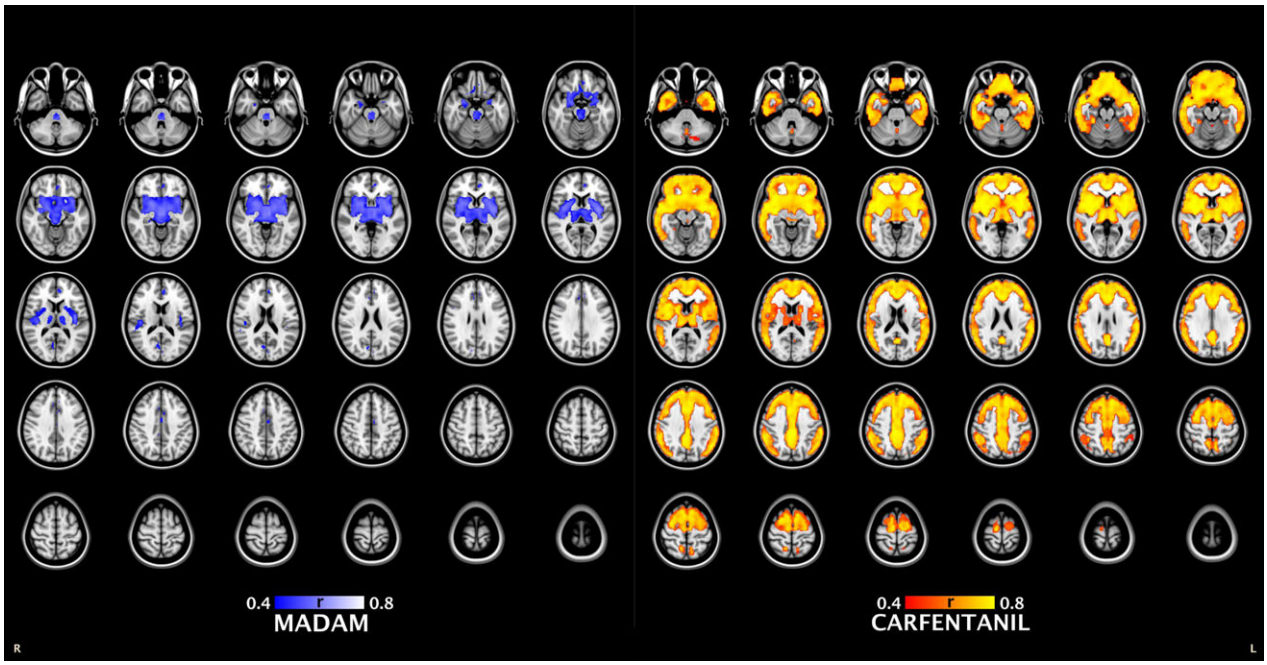

Figure 2.

Axial sections of the brain showing the regions (hubs) with highest intraligand correlation of BP_{ND} for [^{11}C]MADAM (blue to white) on the left panel and for the [^{11}C]carfentanil (red to yellow) on the right panel. In [^{11}C]MADAM, the hub comprised of midbrain, thalamus putamen, caudatus, and amygdala. In [^{11}C]carfentanil, this analysis was unable to differentiate any particular region for being more "connected" with other regions. The data are thresholded at $P < 0.05$ FWE corrected. [Color figure can be viewed in the online issue, which is available at wileyonlinelibrary.com.]

for being more "connected" with other regions. Instead, the cluster (voxel-wise FWE corrected $P < 0.05$, $r > 0.44$) comprised all the regions with nonnegligible [^{11}C]carfentanil BP_{ND}. These results are summarized in Figure 2.

Seed Analysis

Seed analysis was performed only for [^{11}C]MADAM images. An example of seed analysis is given in Supporting Information Figure 1 using midbrain as a seed. BP_{ND}s from the seed ROI correlated only with voxels within the hub regions. That is, no correlation between BP_{ND}s from the seed ROI and voxels that did not belong to the five seed regions was found. Correlations between seed ROIs were statistically significant and coefficients of determinants were high (Fig. 3 and Table I).

Correlation Between [^{11}C]MADAM and [^{11}C]Carfentanil BP_{ND}s

All associations between [^{11}C]MADAM BP_{ND} and [^{11}C]carfentanil BP_{ND} including nonsignificant ones are shown in Figure 4. Both negative and positive correlations coefficients were detected, but only positive correlations were statistically significant (uncorrected voxel-level $P <$

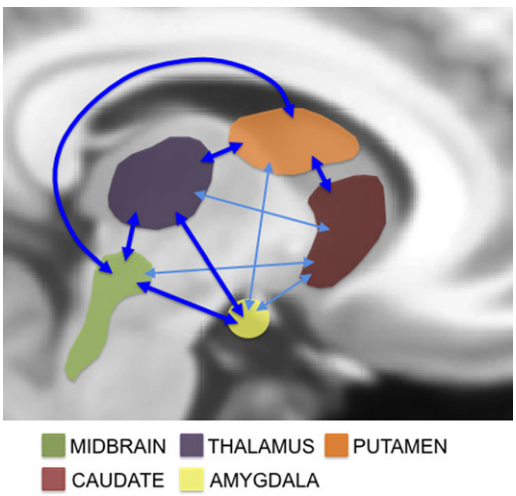

Figure 3.

Summary of the results of the [^{11}C]MADAM seed analysis. Thicker dark blue lines indicate the coefficient of determination above 0.75, thinner light blue lines indicate coefficient of determination between 0.45 and 0.75. Correlation coefficients from these seeds to cortical voxels was below 0.44, indicating that [^{11}C]MADAM BP_{ND} in midbrain or in other parts of this network explained less than 19% of the variance in cortical [^{11}C]MADAM BP_{ND}. [Color figure can be viewed in the online issue, which is available at wileyonlinelibrary.com.]

TABLE I. Regional BP_{ND}s of [^{11}C]MADAM and Pearson correlation coefficients between seed regions

Regions	BP_{ND}[a]	Midbrain	Caudate	Thalamus	Putamen	Amygdala
Midbrain	0.94 ± 0.14	1.00	0.73	0.93	0.86	0.91
Caudate	0.34 ± 0.10	0.73	1.00	0.71	0.88	0.67
Thalamus	0.75 ± 0.11	0.93	0.71	1.00	0.86	0.87
Putamen	0.76 ± 0.13	0.86	0.88	0.86	1.00	0.80
Amygdala	0.58 ± 0.12	0.91	0.67	0.87	0.80	1.00

[a]Mean ± standard deviation.

0.05, $r > 0.44$). These statistically significant correlations were located bilaterally in amygdala, dorsolateral prefrontal cortex, dorsal anterior cingulate cortex, and anteromedial thalamus and unilaterally in the left in parietal and medial temporal cortices (Fig. 5 and Table II).

DISCUSSION

To our knowledge, this is the first study describing correlation between a classical ascending monoamine neurotransmitter system and a modulatory peptide system in vivo in the human brain. We used voxel-wise methods to map intra- and intercorrelations of the [^{11}C]MADAM and [^{11}C]carfentanil BP_{ND} distribution in the brain. As discussed earlier, there are six PET studies investigating the intercorrelations between two different tracers. Five of these studies used only ROI-based approach [Bose et al., 2011; Erritzoe et al., 2010; Jovanovic et al., 2008; Lundberg et al., 2007; Takano et al., 2011] and one study used ROI-derived BP_{ND} in a seed analysis [Cervenka et al., 2010]. Although ROI-based approach is regarded as the gold standard in PET studies, it may be suboptimal when investigating correlation of two different ligands because receptor density does not always follow the anatomically defined boundaries of brain regions [Palomero-Gallagher et al., 2009; Zilles and Amunts, 2009]. Using large ROIs that are differently defined in different studies may also explain some discrepancies of the findings [Bose et al., 2011; Lundberg et al., 2007; Takano et al., 2011]. Our study highlights the feasibility of analyzing voxel-by-voxel associations of BP_{ND} across tracers. This approach may exceed the sensitivity of the ROI-based analysis, particularly in the regions such as the cortical surface that are less susceptible to warping in the normalization step. In comparison to earlier studies, another strength in this study is that both PET scan were done on the same day, whereas only in two of the earlier studies the PET scans were done during the same day [Jovanovic et al., 2008; Lundberg et al., 2007].

Our results suggest that [^{11}C]MADAM and [^{11}C]carfentanil show differential serotonin and opiate network structure, as indicated by different patterns of intraligand correlation of BP_{ND}s. The hub analysis did not differentiate any region as more informative in predicting the overall [^{11}C]carfentanil, BP_{ND} in the brain. Rather, it suggested that any given region in the brain is a good predictor of opiate receptor availability in all the other regions in a "baseline" examination. The hypothesis is that expression of μ-opioid receptors is regulated similarly or by common, e.g., genetic, mechanisms independent of the brain region [Ray et al., 2011].

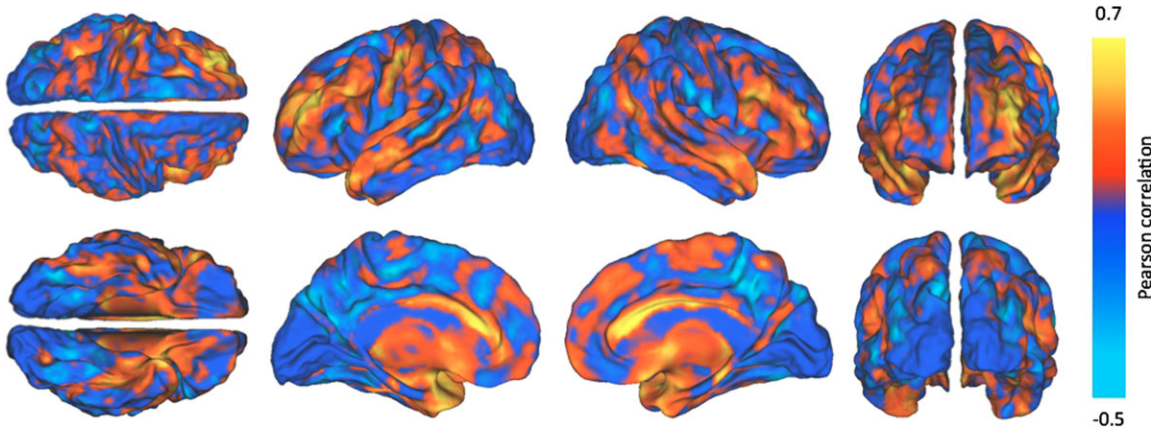

Figure 4.
All voxel-based intercorrelations (Pearson's *r*'s) between [^{11}C]MADAM BPND and [^{11}C]carfentanil BPND. [Color figure can be viewed in the online issue, which is available at wileyonlinelibrary.com.]

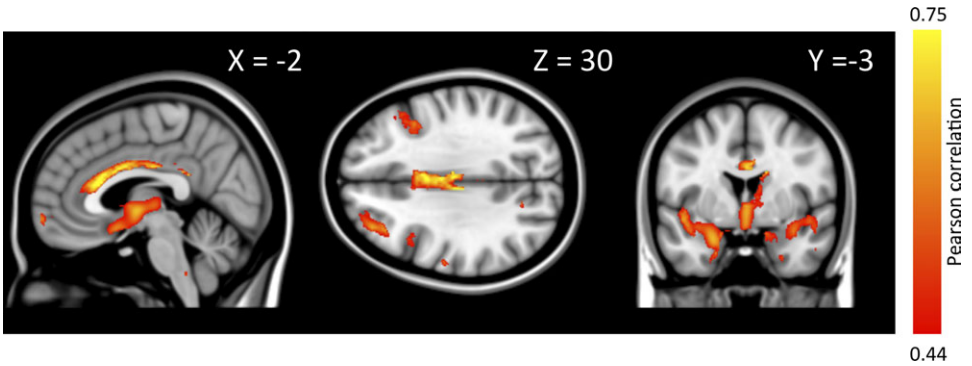

Figure 5.

Sagittal, axial, and coronal sections of the brain showing statistically significant voxel-based intercorrelations (Pearson's *r*'s) between [^{11}C]MADAM BPND and [^{11}C]carfentanil BPND. Correlations are statistically significant in dorsal anterior cingulate cortex, anteromedial thalamus, dorsolateral prefrontal cortex Left parietal cortex, and amygdala when thresholded at $P < 0.05$. [Color figure can be viewed in the online issue, which is available at wileyonlinelibrary.com.]

In contrast, we were able to dissociate five brain regions—midbrain, thalamus, caudatus, putamen, and amygdala—that were highly interconnected but not predictive of [^{11}C]MADAM BP_{ND} in other regions of the brain. These data support the view that there are regional networks within the serotonin system with possible distinct functional relevance. Because the ascending serotonin neurons originate from the midbrain raphe nuclei projecting to both subcortical and cortical regions, one might expect that there is also a link between the levels of midbrain BP_{ND} and cortical BP_{ND}. Perhaps surprisingly, the mean [^{11}C]MADAM BP_{ND} in midbrain was not significantly better predictor of BP_{ND}s in other regions than mean BP_{ND}s in thalamus, caudatus, putamen, or amygdala. Moreover, correlations from midbrain to cortical voxels were not statistically significant even when using very lenient thresholds, i.e., without FWE correction. When interpreting these results, it has to be kept in mind that none of the present serotonin transporter tracers is optimal for quantification of midbrain BP_{ND}. Still, as there was practically no correlation between midbrain and cortex, it is unlikely that this negative finding is entirely due to shortcomings in the imaging technique. Moreover, in the study by Erritzoe et al. [2010], the correlation between midbrain and cortical BP_{ND}s was negligible.

These five regions in the [^{11}C]MADAM hub have high BP_{ND}s [Lundberg et al., 2005] that correspond also to high serotonin transporter density in postmortem study [Varnas et al., 2004]. However, the network did not comprise all regions that have high BP_{ND} and high postmortem serotonin transporter density such as hippocampal complex. This suggests that the network discriminated by the hub analysis is not an artifact related only to high BP_{ND}. [^{11}C]MADAM BP_{ND} is fairly low for most of the cortical regions. Therefore, the lack of intracorrelations could, in principle, be due to lower signal-to-noise ratio. On the other hand, in many regions that did not show up in our "hub" analysis such as anterior cingular cortex test–retest ICC values are as high as in thalamus or striatum [Lundberg et al., 2006]. It should be kept in mind that ICC values in individual voxels are likely to be lower than regional ICC values, although this has not been tested for either ligand.

Moreover, in our data standard deviation of [^{11}C]MADAM BP_{ND} was rather homogeneous across brain regions (data not shown), thus suggesting that the lack of subcortical–cortical correlations is not confounded by low signal-to-noise ratio in the cortex.

Brain networks have most probably a neurodevelopmental basis as suggested for dopamine system [Cervenka et al., 2010]. The effect of genetic polymorphisms on

TABLE II. Peak voxel coordinates and cluster sizes of statistically significant clusters in voxel-wise correlation image between [^{11}C]MADAM and [^{11}C]carfentanil parametric BP_{ND} images

Region	Coordinates (x, y, z)[a]	Cluster size (voxels)
Cingulate cortex[b]	7, −16, 30	2,266
Left amygdale	−39, 2, −16	1,047
Right amygdala	13, −8, −20	714
Right prefrontal cortex	41, 18, 26	237
Left prefrontal cortex	−35, 38, 27	757
Left prefrontal cortex	−33, 6, 42	131
Left parietal cortex	−49, −18, 52	278
Left insula	−45, −24, 16	180

[a]MNI coordinates of the peak voxel.
[b]This cluster extends from cingulate cortex to medial thalamus. Voxel-level threshold of Pearson correlation coefficient r 0.44. Only clusters with more than 100 voxels are shown.

serotonin transporter BP_{ND} has been summarized in a recent review [Willeit and Praschak-Rieder, 2010]. Variability in [^{11}C]DASB BP_{ND} in thalamus may be partly explained by allelic variation in the 5-HT_{2A} receptor gene [Laje et al., 2010], but the findings on the effect of 5-HHTLPR polymorphism on serotonin transporter BP_{ND} are inconsistent [Kobiella et al., 2011; Murthy et al., 2010]. It may be that serotonin transporter density in cortical regions is dependent on different allelic variation than density in subcortical regions or more dependent on interactions with postsynaptic cells and epigenetic modulation and less dependent on neurodevelopmental factors.

To our knowledge, there is only one previous study that has explored within-subject serotonin transporter correlation between regions using [^{11}C]DASB and PET [Erritzoe et al., 2010]. In that study, highest correlations were observed between cortical regions whereas subcortical regions and midbrain had lower correlations with other areas. In this study, we did not examine correlations from cortical seed ROIs as these regions were not in the hub. Our approach differs somewhat from Erritzoe et al's analysis method. Our analysis is tuned toward finding global hubs rather than strong links between specific brain regions, whereas the study by Erritzoe et al. describes a large number of associations between numerous regions. Our approach is data driven and findings are not confined within predefined regions of interest. Furthermore, we used FWE correction in order to distinct the most connected regions, whereas Erritzoe et al. included all correlations. Because of the differences, these two analysis techniques should be considered complementary rather than competing methods for analysis of within neurotransmitter networks.

An entirely novel finding of this study is the correlation between serotonin transporter and μ-opioid receptor. The methodology involves two consecutive tracer injections as close as possible with the interval being determined by ^{11}C- decay. Ideally, the two neurotransmitter systems should be studied simultaneously, but currently there are no suitable imaging methods to overcome this problem. However, same day test–retest studies with these ligands indicate good to excellent reproducibility of the BP_{ND} values in healthy volunteers [Hirvonen et al., 2009; Lundberg et al., 2006]. Consequently, two consecutive injections is a preliminary but feasible approach for our analysis in baseline situations. Another methodological advantage of the current study is that the two tracers used in this study are highly specific to their corresponding target molecules [Edmond et al., 2002; Maguire et al., 1992]. This makes it highly unlikely that [^{11}C]MADAM could bind to μ-opioid receptor or [^{11}C]carfentanil to the serotonin transporter.

Using voxel-based correlation analysis we found brain regions where positive correlations between serotonin transporter and μ-opioid receptor BP_{ND}s were statistically significant: bilaterally anteromedial thalamus, dorsal anterior cingulate cortex, dorsolateral prefrontal cortex, amygdala, and left parietal and medial temporal cortices. BP_{ND} reflects the product of affinity ($1/K_d$) and density (B_{max}), which cannot be separated in a single PET scan. [^{11}C]carfentanil BP_{ND} may be sensitive to endogenous opioid levels [Scott et al., 2007] but in baseline conditions binding potential correlates strongly with B_{max} whereas the correlation between binding potential and K_d is negligible in vivo studies [see Hietala et al., 1999]. We therefore suggest that the high correlation seen between serotonin transporter and μ-opioid receptor BP_{ND}s is mainly due to correlating densities. We speculate that there is a homeostatic mechanism that leads to higher μ-opioid receptor density when serotonin transporter density is high especially in the regions where correlations were high. This may be related to the fact that endogenous opioids are powerful presynaptic modulators of serotonin release [Sbrenna et al., 2000; Tao and Auerbach, 1995, 2002]. We further hypothesize that there are regional differences in how serotonergic neurotransmission is regulated by opioids. This would suggest that especially in regions where correlation was high serotonergic neurotransmission is under opioidergic regulation in healthy humans. A PET study using μ-opioid receptor agonist as a pharmacological challenge and a ligand sensitive to endogenous serotonin levels could test this hypothesis.

Our results serve as a starting point for integrating knowledge from studies where serotonin and opioid systems have been investigated separately in the same condition, e.g., pain in humans. In this work, we have only studied healthy volunteers. It would be important to know whether disease processes alter the association between these neurotransmitters and whether altering one system influences the other. Interplay between neurotransmitters is likely to be of key importance for the function of brain networks as well as some drug effects. For example, μ-opioid receptor knock-out mice do not show typical antidepressant effects to serotonin–noradrenaline reuptake inhibitors [Ide et al., 2010], demonstrating the importance of interplay between monoamine neurotransmitters and μ-opioid receptor for understanding antidepressant effects. Serotonin–noradrenaline reuptake inhibitors are examples of drugs used in psychiatry that affect several different neurotransmitters. Polypharmacy is also commonplace in clinical practice of treating central neural systems diseases. In future, knowledge obtained by studying coexpressions could give better insight to interdependencies between different neurotransmitters as well as mechanisms of action of drugs or combinations of drugs that have many targets. This might help to design more rational drug combination regimes and changes in associations between two neurotransmitters might serve as a surrogate measure for drug effects. A recent study has already investigated such change by demonstrating that connectivity within $5HT_{1A}$ network is affected by selective serotonin reuptake inhibitor treatment [Hahn et al., 2010].

CONCLUSION

We describe methodology for exploring the single or multiple neurotransmitter "connectome" with PET. The value of

these kind of methods will be further enhanced by simultaneous multimodal "system level" functional imaging, e.g., with PET-MRI hybrid cameras. Our study also revealed regional networks within the serotonin system in human brain. That is, serotonin transporter densities in midbrain, thalamus, putamen, caudatus, and amygdala are highly interconnected, as opposed to cortical serotonin transporter. Similar regional or local differences in tracer intracorrelations were not detected within the μ-opioid system.

The main finding of the study is the description of neurotransmitter correlations in specific brain regions/circuits. In our example, association between serotonin and opioid systems was found to be variable in different brain regions. Significant positive correlations were found bilaterally in dorsal anterior cingulate cortex, anteromedial thalamus, dorsolateral prefrontal cortex, and in amygdala and in left parietal cortex. These regions largely overlap with the known network regulating affect and pain. Detailed information on neurotransmitter intercorrelations will be important for etiological questions in neurological and psychiatric disorders. Similarly this approach may offer targets or biomarkers for developing new pharmacotherapy or enhance the understanding how the currently used central nervous system drugs are working.

ACKNOWLEDGMENTS

We thank the staff of Turku PET centre for assistance.

REFERENCES

Bailer UF, Frank GK, Price JC, Meltzer CC, Becker C, Mathis CA, Wagner A, Barbarich-Marsteller NC, Bloss CS, Putnam K, Schork NJ, Gamst A, Kaye WH (2013): Interaction between serotonin transporter and dopamine D2/D3 receptor radioligand measures is associated with harm avoidant symptoms in anorexia and bulimia nervosa. Psychiatry Res. 211:160–168. doi: 10.1016/j.pscychresns.2012.06.010.

Bencherif B, Fuchs PN, Sheth R, Dannals RF, Campbell JN, Frost JJ (2002): Pain activation of human supraspinal opioid pathways as demonstrated by [11C]-carfentanil and positron emission tomography (PET). Pain 99:589–598.

Berger B, Rothmaier AK, Wedekind F, Zentner J, Feuerstein TJ, Jackisch R (2006): Presynaptic opioid receptors on noradrenergic and serotonergic neurons in the human as compared to the rat neocortex. Br J Pharmacol 148:795–806.

Bose SK, Mehta MA, Selvaraj S, Howes OD, Hinz R, Rabiner EA, Grasby PM, Turkheimer FE, Murthy V (2011): Presynaptic 5-HT1A is related to 5-HTT receptor density in the human brain. Neuropsychopharmacology 36:2258–2265.

Cervenka S, Varrone A, Fransen E, Halldin C, Farde L (2010): PET studies of D2-receptor binding in striatal and extrastriatal brain regions: Biochemical support in vivo for separate dopaminergic systems in humans. Synapse 64:478–485.

Comtat C, Bataille F, Michel C, Jones JP, Sibomana M, Janeiro L, Trebossen R (2004): OSEM-3D reconstruction strategies for the ECAT HRRT. Conf Rec 2004 IEEE Nucl Sci Symp Med Imaging Conf 6:3492–3496.

Conturo TE, Lori NF, Cull TS, Akbudak E, Snyder AZ, Shimony JS, McKinstry RC, Burton H, Raichle ME (1999): Tracking neuronal fiber pathways in the living human brain. Proc Natl Acad Sci USA 96:10422–10427.

Emond P, Vercouillie J, Innis R, Chalon S, Mavel S, Frangin Y, Halldin C, Besnard JC, Guilloteau D (2002): Substituted diphenyl sulfides as selective serotonin transporter ligands: synthesis and in vitro evaluation. J Med Chem 45:1253–1258.

Endres CJ, Bencherif B, Hilton J, Madar I, Frost JJ (2003): Quantification of brain mu-opioid receptors with [11C]carfentanil: reference-tissue methods. Nucl Med Biol 30:177–186.

Erritzoe D, Holst K, Frokjaer VG, Licht CL, Kalbitzer J, Nielsen FA, Svarer C, Madsen J, Knudsen G (2010): A nonlinear relationship between cerebral serotonin transporter and 5-HT(2A) receptor binding: An in vivo molecular imaging study in humans. J Neurosci 30:3391–3397.

Frost JJ, Wagner HN Jr, Dannals RF, Ravert HT, Links JM, Wilson AA, Burns HD, Wong DF, McPherson RW, Rosenbaum AE (1985): Imaging opiate receptors in the human brain by positron tomography. J Comput Assist Tomogr 9:231–236.

Gunn RN, Lammertsma AA, Hume SP, Cunningham VJ (1997): Parametric imaging of ligand-receptor binding in PET using a simplified reference region model. Neuroimage 6:279–287.

Hahn A, Lanzenberger R, Wadsak W, Spindelegger C, Moser U, Mien LK, Mitterhauser M, Kasper S (2010): Escitalopram enhances the association of serotonin-1A autoreceptors to heteroreceptors in anxiety disorders. J Neurosci 30:14482–14489.

Hietala J, Någren K, Lehikoinen P, Ruotsalainen U, Syvälahti E (1999): Measurement of striatal D2 dopamine receptor density and affinity with [11C]-raclopride in vivo: A test-retest analysis. J Cereb Blood Flow Metab 19(2):210–217.

Hirvonen J, Hietala J (2011): Dysfunctional brain networks and genetic risk for schizophrenia: Specific neurotransmitter systems. CNS Neurosci Ther 17:89–96.

Hirvonen J, Aalto S, Hagelberg N, Maksimow A, Ingman K, Oikonen V, Virkkala J, Nagren K, Scheinin H (2009): Measurement of central mu-opioid receptor binding in vivo with PET and [11C]carfentanil: A test-retest study in healthy subjects. Eur J Nucl Med Mol Imaging 36:275–286.

Hirvonen M, Laakso A, Nagren K, Rinne JO, Pohjalainen T, Hietala J (2004): C957T polymorphism of the dopamine D2 receptor (DRD2) gene affects striatal DRD2 availability in vivo. Mol Psychiatry 9:1060–1061.

Hirvonen MM, Lumme V, Hirvonen J, Pesonen U, Nagren K, Vahlberg T, Scheinin H, Hietala J (2009): C957T polymorphism of the human dopamine D2 receptor gene predicts extrastriatal dopamine receptor availability in vivo. Prog Neuropsychopharmacol Biol Psychiatry 33:630–636.

Ide S, Fujiwara S, Fujiwara M, Sora I, Ikeda K, Minami M, Uhl GR, Ishihara K (2010): Antidepressant-like effect of venlafaxine is abolished in mu-opioid receptor-knockout mice. J Pharmacol Sci 114:107–110.

Jovanovic H, Lundberg J, Karlsson P, Cerin A, Saijo T, Varrone A, Halldin C, Nordstrom AL (2008): Sex differences in the serotonin 1A receptor and serotonin transporter binding in the human brain measured by PET. Neuroimage 39:1408–1419.

Kobiella A, Reimold M, Ulshöfer DE, Ikonomidou VN, Vollmert C, Vollstädt-Klein S, Rietschel M, Reischl G, Heinz A, Smolka MN (2011): How the serotonin transporter 5-HTTLPR polymorphism influences amygdala function: The roles of in vivo

serotonin transporter expression and amygdala structure. Transl Psychiatry 1:e37.
Laje G, Cannon DM, Allen AS, Klaver JM, Peck SA, Liu X, Manji HK, Drevets WC, McMahon FJ (2010): Genetic variation in HTR2A influences serotonin transporter binding potential as measured using PET and [11C]DASB. Int J Neuropsychopharmacol 13:715–724.
Lammertsma AA, Hume SP (1996): Simplified reference tissue model for PET receptor studies. Neuroimage 4:153–158.
Liberzon I, Zubieta JK, Fig LM, Phan KL, Koeppe RA, Taylor SF (2002): mu-Opioid receptors and limbic responses to aversive emotional stimuli. Proc Natl Acad Sci USA 99:7084–7089.
Lopez-Gimenez JF, Vilaro MT, Milligan G (2008): Morphine desensitization, internalization, and down-regulation of the mu opioid receptor is facilitated by serotonin 5-hydroxytryptamine2A receptor coactivation. Mol Pharmacol 74:1278–1291.
Lundberg J, Odano I, Olsson H, Halldin C, Farde L (2005): Quantification of 11C-MADAM binding to the serotonin transporter in the human brain. J Nucl Med 46:1505–1515.
Lundberg J, Halldin C, Farde L (2006): Measurement of serotonin transporter binding with PET and [11C]MADAM: A test-retest reproducibility study. Synapse 60:256–263.
Lundberg J, Borg J, Halldin C, Farde L (2007): A PET study on regional coexpression of 5-HT1A receptors and 5-HTT in the human brain. Psychopharmacology (Berl) 195:425–433.
Maguire P, Tsai N, Kamal J, Cometta-Morini C, Upton C, Loew G (1992): Pharmacological profiles of fentanyl analogs at mu, delta and kappa opiate receptors. Eur J Pharmacol 213:219–225.
Maldjian JA, Laurienti PJ, Kraft RA, Burdette JH (2003): An automated method for neuroanatomic and cytoarchitectonic atlas-based interrogation of fMRI data sets. Neuroimage 19:1233–1239.
Marsman A, van den Heuvel MP, Klomp DW, Kahn RS, Luijten PR, Hulshoff Pol HE (2013): Glutamate in schizophrenia: A focused review and meta-analysis of 1H-MRS studies Schizophr Bull 39:120–129. doi: 10.1093/schbul/sbr069.
Martikainen IK, Hirvonen J, Kajander J, Hagelberg N, Mansikka H, Nagren K, Hietala J, Pertovaara A (2007): Correlation of human cold pressor pain responses with 5-HT(1A) receptor binding in the brain. Brain Res 1172:21–31.
Mayberg HS (1997): Limbic-cortical dysregulation: A proposed model of depression. J Neuropsychiatry Clin Neurosci 9:471–481.
Meyer JH (2007): Imaging the serotonin transporter during major depressive disorder and antidepressant treatment. J Psychiatry Neurosci 32:86–102.
Moore RY, Halaris AE, Jones BE (1978): Serotonin neurons of the midbrain raphe: ascending projections. J Comp Neurol 180:417–438.
Murthy NV, Selvaraj S, Cowen PJ, Bhagwagar Z, Riedel WJ, Peers P, Kennedy JL, Sahakian BJ, Laruelle MA, Rabiner EA, Grasby PM (2010): Serotonin transporter polymorphisms (SLC6A4 insertion/deletion and rs25531) do not affect the availability of 5-HTT to [11C] DASB binding in the living human brain. Neuroimage 52:50–54.
Nakamura K, Sekine Y, Ouchi Y, Tsujii M, Yoshikawa E, Futatsubashi M, Tsuchiya KJ, Sugihara G, Iwata Y, Suzuki K, Matsuzaki H, Suda S, Sugiyama T, Takei N, Mori N (2010): Brain serotonin and dopamine transporter bindings in adults with high-functioning autism. Arch Gen Psychiatry 67:59–68.
Palomero-Gallagher N, Vogt BA, Schleicher A, Mayberg HS, Zilles K (2009): Receptor architecture of human cingulate cortex: Evaluation of the four-region neurobiological model. Hum Brain Mapp 30:2336–2355.
Price JL, Drevets WC (2010): Neurocircuitry of mood disorders. Neuropsychopharmacology 35:192–216.
Rahmim A, Cheng JC, Blinder S, Camborde ML, Sossi V (2005): Statistical dynamic image reconstruction in state-of-the-art high-resolution PET. Phys Med Biol 50:4887–4912.
Raichle ME, MacLeod AM, Snyder AZ, Powers WJ, Gusnard DA, Shulman GL (2001): A default mode of brain function. Proc Natl Acad Sci USA 98:676–682.
Ray R, Ruparel K, Newberg A, Wileyto EP, Loughead JW, Divgi C, Blendy JA, Logan J, Zubieta JK, Lerman C (2011): Human Mu Opioid Receptor (OPRM1 A118G) polymorphism is associated with brain mu-opioid receptor binding potential in smokers. Proc Natl Acad Sci USA 108:9268–9273.
Sbrenna S, Marti M, Morari M, Calo G, Guerrini R, Beani L, Bianchi C (2000): Modulation of 5-hydroxytryptamine efflux from rat cortical synaptosomes by opioids and nociception. Br J Pharmacol 130:425–433.
Scott D, Stohler, C, Koeppe R, Zubieta J (2007): Time-course of change in [11C]carfentanil and [11C]raclopride binding potential after a nonpharmacological challenge. Synapse 61:707–714.
Simmons ML, Chavkin C (1996): Endogenous opioid regulation of hippocampal function. Int Rev Neurobiol 39:145–196.
Sporns O, Tononi G, Kotter R (2005): The human connectome: A structural description of the human brain. PLoS Comput Biol 1:e42.
Takano H, Ito H, Takahashi H, Arakawa R, Okumura M, Kodaka F, Otsuka T, Kato M, Suhara T (2011): Serotonergic neurotransmission in the living human brain: A positron emission tomography study using [(11)C]dasb and [(11)C]WAY100635 in young healthy men. Synapse 65:624–633.
Tao R, Auerbach SB (1995): Involvement of the dorsal raphe but not median raphe nucleus in morphine-induced increases in serotonin release in the rat forebrain. Neuroscience 68:553–561.
Tao R, Auerbach SB (2002): Opioid receptor subtypes differentially modulate serotonin efflux in the rat central nervous system. J Pharmacol Exp Ther 303:549–556.
Tarkiainen J, Vercouille J, Emond P, Sandell J, Hiltunen J, Frangin Y, Guilloteau D, Halldin C (2001): Carbon-11 labelling of MADAM in two different positions: A highly selective PET radioligand for the serotonin transporter. J Labelled Compd Radiopharm 44:1013–1023.
Varnas K, Halldin C, Hall H (2004): Autoradiographic distribution of serotonin transporters and receptor subtypes in human brain. Hum Brain Mapp 22:246–260.
Willeit M, Praschak-Rieder N (2010): Imaging the effects of genetic polymorphisms on radioligand binding in the living human brain: A review on genetic neuroreceptor imaging of monoaminergic systems in psychiatry. Neuroimage 53:878–892.
Zilles K, Amunts K (2009): Receptor mapping: Architecture of the human cerebral cortex. Curr Opin Neurol 22:331–339.